

5. Y. Syono and T. Goto, *Sci. Rep. Res. Inst. Tohoku Univ. Ser. A* **29**, 17 (1980).
6. H. Takei and T. Kobayashi, *J. Cryst. Growth* **23**, 121 (1974).
7. The electron microscopy observations were carried out with 200- and 1000-kV TEM at Tohoku University and 100-kV analytical TEM at Osaka University.
8. L. Liu, *Geophys. Res. Lett.* **2**, 417 (1975); *Nature (London)* **262**, 770 (1976); E. Ito, *Geophys. Res. Lett.* **4**, 72 (1977).
9. Y. Matsui and K. Kawamura, *Nature (London)* **285**, 648 (1980); Y. Matsui *et al.*, in *High-Pressure Research in Geophysics*, S. Akimoto and M. H. Manghnani, Eds. (Center for Academic Publications Japan, Tokyo, in press).
10. D. E. Grady, in *High-Pressure Research: Applications in Geophysics*, M. H. Manghnani and S. Akimoto, Eds. (Academic Press, New York, 1977), p. 389.
11. Y. Syono and T. Goto, in *High-Pressure Research in Geophysics*, S. Akimoto and M. H. Manghnani, Eds. (Center for Academic Publications Japan, Tokyo, in press).
12. We benefited from invaluable discussions with Y. Matsui, Okayama University, and I. Kushi, University of Tokyo. We thank H. Ohta and E. Aoyagi for technical assistance with the TEM observations and J. Sato and H. Moriya for assistance with preparation of the manuscript. Work supported by Grant in Aid for Special Project Research (321503, 420902, and 510104) given by the Ministry of Education, Science and Culture.

23 March 1981; revised 16 June 1981

Axonal Transport: Each Major Rate Component Reflects the Movement of Distinct Macromolecular Complexes

Abstract. *The proteins of the three major rate components of axonal transport in guinea pig retinal ganglion cells were analyzed by one- and two-dimensional gel electrophoresis. Each rate component consisted of a different set of proteins that remained associated with each other during transport. This suggests that each rate component represents a distinct macromolecular complex and that these complexes may be definable organelles such as microtubules, microfilaments, and smooth endoplasmic reticulum. Thus, the transport of radiolabeled proteins in the axon reflects the movement of complete subcellular structures rather than the movement of individual proteins.*

The axon and its terminal depend on the continuous delivery of proteins synthesized in the cell body to maintain their structural and functional integrity. Axonal proteins leave the cell body as five separate groups, each different and moving at a distinct rate (1-7). Some of these proteins have been associated with specific structures in the axon, such as microtubules, neurofilaments, microfilaments, and mitochondria (2-3, 8). These observations led us to propose a structural hypothesis of axonal transport: proteins are transported in the axon as component parts of intact cytological structures.

Axonal transport was studied in Hartley guinea pig hypoglossal and retinal ganglion cells. The long hypoglossal axons were used to study the kinetics of transport, and the retinal ganglion cell proteins, which could be radiolabeled to high specific activities, were used for more detailed analyses. Transported proteins were labeled by injecting 100 to 500 μ Ci of either [35 S]methionine or a 1:1 mixture of [3 H]lysine and [3 H]proline into the hypoglossal nucleus or the posterior chamber of the eye (2, 9). At various times thereafter the labeled nerves were removed. The hypoglossal nerve was cut into 3-mm segments, and the radioactive proteins of each rate component of axonal transport were precipitated from the segments with trichloroacetic acid. The polypeptides in each wave were analyzed in segments of

optic nerve and tract by sodium dodecyl sulfate-polyacrylamide gel electrophoresis (SDS-PAGE) alone or in combination with isoelectric focusing (two-dimensional PAGE) (10). Gels were stained with Coomassie blue and radioactive

proteins were detected by fluorography (11).

Three waves of labeled proteins correspond to the major rate components of axonal transport in the hypoglossal nerve (Fig. 1). One wave, present 3 hours after the injection of 3 H-labeled amino acids, corresponds to the fast component (FC), which moves at about 400 mm/day. Two other waves, one in the proximal portion and one in the distal portion of the nerve 15 days after the injection of 3 H-labeled amino acids, correspond respectively to slow component a (SCa), moving at 0.3 to 1.0 mm/day, and slow component b (SCb), moving at 2 to 4 mm/day (1, 3, 9). By selecting the injection and analysis intervals appropriately, it is possible to resolve SCa, SCb, and FC from each other and analyze separately the proteins in each rate component. Two other components of axonal transport, which have rates intermediate to those of FC and SCb (6) and represent a much smaller proportion of the total transported radioactivity than that of SCa, SCb, and FC, are not included in this analysis (6, 12).

The SDS-PAGE analyses of SCa, SCb, and FC (Fig. 2) show that most of the radioactive bands are present in just one of the three components (13), but the resolution is insufficient to unequivocally demonstrate that each polypeptide is present in only one rate component. For example, there is an overlap of bands in SCb and FC with molecular weights between 47,000 and 92,000. To resolve these overlapping bands the polypeptides comprising SCa, SCb, and FC were analyzed by two-dimensional PAGE, which separates polypeptides of similar molecular weight by their differences in charge (10). The results (Fig. 3) show that, with only one possible exception [the polypeptide enclosed by parentheses in the fluorographs of SCa and SCb (Fig. 3)], each of the more than 100 polypeptides detected is present in only one rate component. This indicates that SCa, SCb, and FC each consists of distinct polypeptides. Earlier SDS-PAGE studies (1-3, 8) showed that different polypeptides are transported at each of the five rates but did not reveal the distinctive composition of each rate component. The pattern of spots produced by two-dimensional PAGE (Fig. 3) may be used to identify and rigorously define the protein composition of each rate component.

Any model to explain axonal transport must now account for the segregation of the proteins in one rate component apart from those in other rate components as they move past one another. Some cur-

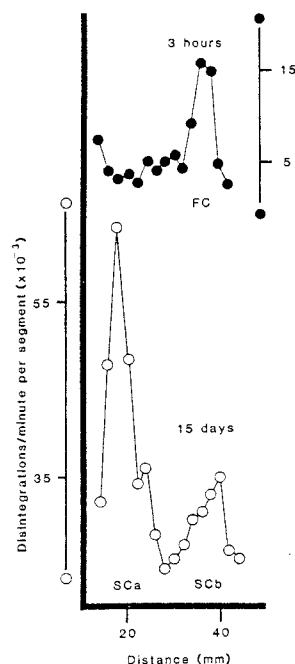


Fig. 1. The distribution of radioactive proteins in the hypoglossal nerves of two guinea pigs 3 hours or 15 days after an injection of 3 H-labeled amino acids. The scale of disintegrations per minute per segment is on the right for FC and on the left for SCa and SCb. The distance is measured from the hypoglossal nucleus.

rent models (14, 15) do not account for this observation. The results of our analyses can be explained by a model of axonal transport in which each rate component represents a discrete macromolecular assembly that moves as a unit. The structural hypothesis provides such a model, in that it holds that a particular protein is conveyed in the axon either as an integral part of a moving cytological structure or in long-term association with one of those structures.

On the basis of current literature, it appears that each major rate component can now be related to a particular cytological structure. The fast component, which is characterized by its membrane-associated proteins and its lipids, corresponds to the tubulovesicular compartment of the axon. These membranous structures are probably synthesized on the rough endoplasmic reticulum, processed through the Golgi complex (16), and then transported anterogradely in the axon as vesicles, dense core granules, and membranous tubules (4, 8, 17-19). After reaching the axon terminal, some of these materials may return to the cell body by retrograde transport as multivesicular and lamellar bodies that eventually interact with lysosomes in the

cell body (19, 20). The two slow components of axonal transport are characterized by the presence of cytoskeletal proteins: SCa has been related to the microtubule-neurofilament network, and SCb may correspond to actin containing microfilaments and the associated axoplasmic matrix (21). If, as we propose, each group of proteins corresponds to a specific structure, then the movement of the proteins in each group will be determined by the motile properties of that structure. In our model, the proteins constituting FC are rapidly transported because they are part of the set of discrete membranous vesicles that move rapidly. Similarly, the proteins of SCa and SCb move at much slower rates because of the motility of the cytoskeletal elements. The slower rates of axonal transport are similar to the rates at which some cells move and axons elongate during development or regeneration (22).

The structural hypothesis does not preclude the existence of interactions between the proteins of different rate components. Certain proteins in each complex may interact with those in other complexes to produce the different rates and directions of movement in the axon.

Such proteins would be recognizable by their appearance in more than one rate component. Although few proteins exhibit such behavior in retinal ganglion cells, an example is the protein with molecular weight 230,000 that appears in both SCa and SCb (see parentheses in Fig. 3) (23).

Remarkably, the coherent transport of proteins as part of specific axonal structures extends to the soluble proteins of the neuron, which have been thought to be freely diffusible. For example, calmodulin and nerve-specific enolase are both readily solubilized from the nervous tissue, but these and many other soluble proteins are transported coherently in association with the SCb structures (24). Thus both calmodulin and enolase have a preferential affinity for the structural complex represented by SCb. The nature of the cytological structure that can encompass the wide variety of easily solubilized proteins that are coherently transported as SCb is enigmatic. However, Ellisman and Porter (25) identified a highly ordered trabecular structure in the axoplasmic ground substance that might represent the structural assemblies of soluble proteins that correspond to SCb.

Our observations that proteins are

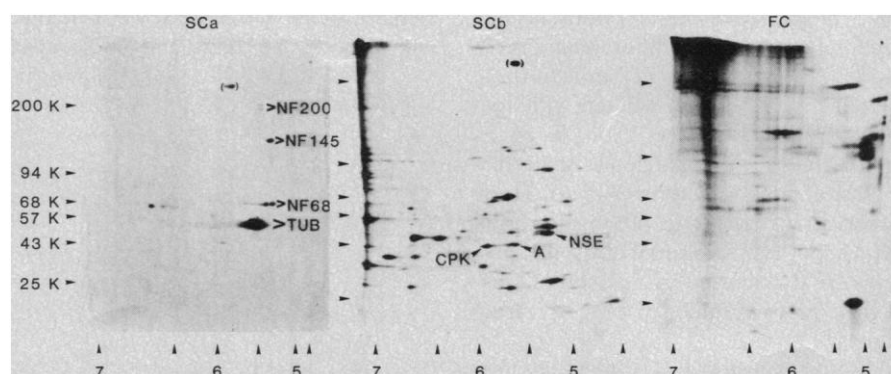
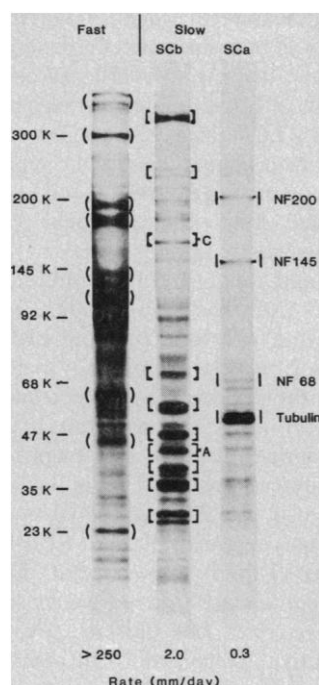


Fig. 2 (left). A comparison of the labeled polypeptides constituting the fast component and slow components (SCa and SCb) of axonal transport in retinal ganglion cells. The symbols enclosing specific bands in each column indicate those polypeptides that appear to be distinct to each component on the basis of multiple analyses. The radioactive bands below tubulin in the SCb profile are not SCa polypeptides but represent the trailing portion of the wave of SCb polypeptides (26). Known polypeptides are indicated: C is clathrin (27); A is actin (2, 9); NF 68, 145, and 200 are the neurofilament polypeptides (1, 3, 9); and tubulin is α - and β -tubulin (1, 3, 9). Each component was radioactively labeled in a separate guinea pig with [3 H]lysine and [3 H]proline (1:1). To increase the yield of labeled fast transported proteins, the optic nerve was cut proximal to the chiasm just before the injection of 3 H-labeled amino acids. This procedure causes no detectable changes in the labeled proteins observed when compared with the intact nerve (28). Segments (2 to 5 mm) of optic nerve, tract, or both containing the labeled proteins were removed from guinea pigs after 6 hours (FC), 6 days (SCb), or 38 days (SCa) and

processed for SDS-PAGE. Fig. 3 (right). Fluorographs of the two-dimensional gels of the polypeptides of the three major components of axonal transport in retinal ganglion cells. Isoelectric focusing was performed horizontally (approximate pH gradient is indicated along the bottom of each gel) and SDS-PAGE was performed vertically (apparent molecular weight is indicated to the left of each gel). Tubulin (TUB) and the neurofilament polypeptides (NF 68, 145, and 200) are identified in the gel of SCa; NF 200 is a doublet in some of the guinea pigs of the strain used. In the gel of SCb, the known proteins are nerve-specific enolase (NSE) and creatine phosphokinase (CPK) (24), in addition to actin (A). Clathrin is not indicated because it forms a streak that is too faint to be seen (28). Because these fluorographs were exposed for long periods to show minor polypeptides, small amounts of radioactivity corresponding to the tubulins and NF 68 were detected in the SCb fluorograph; this represents overlap of the leading edge of SCa with the trailing part of SCb (29). The smearing of spots in the FC pattern appears to be characteristic of glycoproteins (30). Each component was labeled as described in the legend to Fig. 2, except that [35 S]methionine was used. The gels were exposed to the film for times sufficient to detect a polypeptide focused into a spot of 1 mm² and containing as little as 0.9, 0.3, or 0.1 disintegrations per minute for the fluorographs of SCa, SCb, and FC, respectively (11).

transported in segregated rate classes, each with a distinctive composition, supports the structural hypothesis of axonal transport. Furthermore, these observations are part of a growing body of data that indicate that the biologically relevant units of axonal transport are likely to be cytological structures and not individual protein molecules.

MICHAEL TYTELL

Department of Anatomy,
Bowman Gray School of Medicine,
Winston-Salem, North Carolina 27103

MARK M. BLACK

Department of Anatomy,
Temple University Medical Center,
Philadelphia, Pennsylvania 19104

JUDY A. GARNER

Department of Microbiology,
School of Medicine,
Case Western Reserve University,
Cleveland, Ohio 44106

RAYMOND J. LASEK

Department of Anatomy,
School of Medicine,
Case Western Reserve University

References and Notes

1. P. N. Hoffman and R. J. Lasek, *J. Cell Biol.* **66**, 351 (1975).
2. M. M. Black and R. J. Lasek, *Brain Res.* **171**, 401 (1979).
3. ———, *J. Cell Biol.* **86**, 616 (1980).
4. G. C. Stone, D. L. Wilson, M. E. Hall, *Brain Res.* **144**, 287 (1978).
5. D. L. Wilson and G. C. Stone, *Annu. Rev. Biophys. Bioeng.* **8**, 27 (1979).
6. M. B. Willard, W. M. Cowan, P. R. Vagelos, *Proc. Natl. Acad. Sci. U.S.A.* **71**, 2183 (1974).
7. M. B. Willard and K. L. Hulebak, *Brain Res.* **136**, 289 (1977).
8. T. Lorenz and M. Willard, *Proc. Natl. Acad. Sci. U.S.A.* **75**, 505 (1978).
9. M. M. Black and R. J. Lasek, *J. Neurobiol.* **9**, 433 (1978).
10. U. K. Laemmli, *Nature (London)* **227**, 680 (1970); P. H. O'Farrell, *J. Biol. Chem.* **250**, 4007 (1975).
11. W. M. Bonner and R. A. Laskey, *Eur. J. Biochem.* **46**, 83 (1974); R. A. Laskey and A. D. Mills, *ibid.* **56**, 335 (1975).
12. M. Tytell, unpublished data. Analyses of the intermediate components (M. Tytell and R. J. Lasek, in preparation) support the structural hypothesis.
13. Similar observations have been made in hypoglossal axons (M. M. Black, unpublished data). The interpretations of the gels in Figs. 2 and 3 are based on analyses of many such gels. Variations from one gel to another were compensated for by relating the positions of radioactive bands and spots to the positions of molecular weight standards and the major proteins of the axon revealed by Coomassie blue staining of each gel.
14. S. Ochs, in *Third International Congress on Muscle Disease*, W. G. Bradley, D. Gardner-Medwin, J. N. Walton, Eds. (Excerpta Medica, Amsterdam, 1975), vol. 360, p. 189.
15. G. W. Gross, *Adv. Neurol.* **12**, 283 (1975).
16. B. Droz, in *The Nervous System*, vol. 1, *Basic Neurosciences*, D. B. Tower, Ed. (Raven, New York, 1975), p. 111; R. Hammerschlag, G. C. Stone, F. A. Bolen, *Trans. Am. Soc. Neurochem.* **12**, 144 (1981).
17. G. Bennett, L. Di Giamberardino, H. L. Koenig, B. Droz, *Brain Res.* **60**, 129 (1973); L. Di Giamberardino, G. Bennett, H. L. Koenig, B. Droz, *ibid.*, p. 147; B. Droz, H. L. Koenig, L. Di Giamberardino, *ibid.*, p. 93; M. Willard, M. Wiseman, J. Levine, P. Skene, *J. Cell Biol.* **81**, 581 (1979).
18. J. Zelená, A. Lubińska, E. Butmann, *Z. Zellforsch. Mikrosk. Anat.* **91**, 200 (1968).
19. S. Tsukita and H. Ishikawa, *J. Cell Biol.* **84**, 513 (1980).
20. E. Holtzman, *Philos. Trans. R. Soc. London Ser. B* **261**, 407 (1971); J. H. LaVail and M. M.

- LaVail, *J. Comp. Neurol.* **157**, 303 (1974); M. M. LaVail and J. H. LaVail, *Brain Res.* **85**, 273 (1975); R. S. Smith, *J. Neurocytol.* **7**, 611 (1978).
21. The data in (1, 3) indicate that there is little turnover of axonal proteins as they are transported.
22. L. Lubińska, *Prog. Brain Res.* **13**, 1 (1964); E. W. Taylor, *Neurosci. Res. Program Bull.* **19**, 136 (1981).
23. This polypeptide is probably identical to the polypeptide called fodrin by J. Levine and M. Willard [*Soc. Neurosci. Abstr.* **5**, 61 (1979); *J. Cell Biol.* **87**, 206a (1980)].
24. S. T. Brady and R. J. Lasek, *Cell* **23**, 515 (1981).
25. M. H. Ellisman and K. R. Porter, *J. Cell Biol.* **87**, 464 (1980).
26. Because SCb contains about five times more radioactivity than SCa in retinal ganglion cell axons, some of the more intensely labeled SCb polypeptides can still be detected in those axons after the wave of labeled SCa polypeptides has entered (3).

27. J. A. Garner and R. J. Lasek, *J. Cell Biol.* **88**, 172 (1981).
28. M. Tytell, unpublished observation.
29. J. A. Garner, thesis, Case Western Reserve University (1978).
30. The poor resolution of FC proteins is probably due to the fact that most of them are glycosylated. Glycoproteins are known to bind SDS anomalously [R. Pitt-Rivers and F. S. A. Impiombato, *Biochem. J.* **109**, 825 (1968); K. Weber and M. Osborn, in *The Proteins*, H. Neurath and R. L. Hill, Eds. (Academic Press, New York, 1975), vol. 1, p. 179].
31. We acknowledge the excellent technical contributions of S. Ricketts and D. Filsinger and thank S. T. Brady, M. J. Katz, and I. G. McQuarrie for their helpful comments. This work was supported by NIH grants NS 14900-02 and NS 13658-03 awarded to R.J.L. and NIH postdoctoral fellowship NS 05892-02 awarded to M.T.

30 June 1980; revised 4 May 1981

Changes in Sediment Storage in the Coon Creek Basin, Driftless Area, Wisconsin, 1853 to 1975

Abstract. For any time period, total basin sediment yield can be used to make reliable estimates of upland erosion rates only when no significant change in sediment storage is in progress. In the case of Coon Creek, almost 50 percent of human-induced sediment has historically gone into floodplain storage and less than 7 percent has left the basin. However, some of the stored sediment is becoming mobile, and the present yield per unit area may actually be increasing downstream with the augmentation coming from the storage loss.

Sediment yield is much less sensitive than change of sediment storage as an indicator of environmental change in some highly impacted stream basins (1). Because of these storage changes, there may be a poor correlation between material supplied to the stream by upland erosion and sediment yield at the lower end of the basin. These findings reinforce conclusions drawn from earlier research in the southeastern United States (2).

A sediment budget was constructed for Coon Creek, a drainage basin of 360 km² in the Driftless Area of southwestern Wisconsin for two periods: 1853 to 1938 and 1938 to 1975 (Fig. 1). Investigators measured the storage of modern sediment (since 1853) during the period 1974 through 1979, using techniques described in (3). Most storage is along streams, with alluvial deposits in the main valley accounting for about 75 percent of all measured sediment in the basin.

The sediment yield of Coon Creek since the beginning of agricultural activity was estimated on the basis of reservoir sedimentation rates from the nearby, physically and agriculturally similar Beaver Creek Basin. The reservoir on Beaver Creek was built in 1867, and total sediment accumulation was measured in 1939 (4) and in 1976–1977. The accumulation for both time periods was adjusted by means of the Brune trap efficiency curve (5) to estimate sediment inflow.

Total sheet and rill erosion since 1853 was estimated by applying the universal soil loss equation (6, 7) at different dates and integrating the rates. Upland gully erosion was estimated by subtracting, during the period of peak erosion and sedimentation, the sum of the rates of upland sheet and rill erosion and the measured tributary erosion (3) from the sum of the rates of storage gain and sediment yield. This estimate is a minimal value: gully erosion was probably a greater proportion of the total erosion than indicated in Fig. 1. The overall average depth of erosion for 1853 to 1975 is 13.2 cm and compares well with 9.3 cm from an earlier estimate (8), which was based on soil-profile truncations and on consideration of sheet erosion on open pasture and cultivated land. Had woodland and gully erosion been included, the two estimates would have been closer.

Colluvium is the residual after the sum of storage gain and sediment yield is subtracted from total erosion. It is the least reliably quantified component of the sediment budget.

The most significant pattern to emerge from this sediment budget is that sediment yield has been small compared with either erosion or change in sediment storage. In view of the fact that so much emphasis has been placed on sediment yield as an indicator of erosional processes (2), it is instructive to realize that in this area sediment yield was only about 6 percent of all upland erosion